

## Article

# A Study on the Evacuation of an Extra-Long Highway Tunnel Fire—A Case Study of Chengkai Tunnel

Kai Wang <sup>1,2,\*</sup>, Jingwei Hu <sup>1</sup>, Ruiding Chen <sup>1</sup> and Jianhua Wang <sup>1</sup><sup>1</sup> School of Safety Engineering, China University of Mining and Technology, Xuzhou 221116, China<sup>2</sup> Jiangsu Key Laboratory of Fire Safety in Urban Underground Space, Xuzhou 221116, China

\* Correspondence: wangkaifirst@cumt.edu.cn

**Abstract:** The smoke from tunnel fires spreads over long distances and is difficult to vent. Smoke accumulation leads to high temperatures, low visibility, and high concentrations of toxic gases, which greatly hinders the evacuation of people inside the tunnel. In this paper, a representative extra-long highway tunnel—Chengkai Tunnel—is selected as the engineering background, and a tunnel model is built using FDS and Pathfinder software to simulate the fire scenario and evacuation scenario under different longitudinal wind speeds. The concept of safe evacuation reliability is proposed to describe the relationship between the ASET (available safe egress time) and the RSET (required safe egress time). The simulation results show that with the increase in longitudinal wind speed, the ASET upstream of fire source increases first and then remains unchanged, while ASET downstream of fire source increases first and then decreases. The ASET upstream of the fire source is affected by visibility, while the ASET downstream of the fire source is affected by visibility when the wind speed is low, and is affected by temperature as the wind speed increases. The bottleneck effect is an important reason for the long evacuation time of people. The blockage time is a power function of the evacuation movement time, and increasing the width of the cross passage can improve the evacuation efficiency of the tunnel. The increase in the number of evacuees will reduce the reliability of the safe evacuation of personnel. Among all simulated scenarios, a longitudinal wind speed of 2.5 m/s has the highest safe evacuation reliability, with 0.79, 0.92, and 0.99 for scenarios R1, R2, and R3, respectively. Excessive wind speed reduces the safe evacuation reliability downstream of the fire source.



**Citation:** Wang, K.; Hu, J.; Chen, R.; Wang, J. A Study on the Evacuation of an Extra-Long Highway Tunnel Fire—A Case Study of Chengkai Tunnel. *Sustainability* **2023**, *15*, 4865. <https://doi.org/10.3390/su15064865>

Academic Editor: Fuqiang Yang

Received: 25 November 2022

Revised: 1 March 2023

Accepted: 3 March 2023

Published: 9 March 2023



**Copyright:** © 2023 by the authors. Licensee MDPI, Basel, Switzerland. This article is an open access article distributed under the terms and conditions of the Creative Commons Attribution (CC BY) license (<https://creativecommons.org/licenses/by/4.0/>).

**Keywords:** extra-long highway tunnel; tunnel evacuation; ASET; RSET; safety evacuation reliability

## 1. Introduction

Tunnels are one of the important infrastructures to build highway transportation networks. With the rapid development of traffic construction, more and more highway tunnels are being built, and they are getting longer and longer. By the end of 2020, the number of highway tunnels in China was 21,316, up 10.6% year-on-year. The total length of tunnels reached 21.993 million meters, an increase of 13.8% year-on-year. It is worth noting that the length of extra-long road tunnels ( $\geq 3$  km) accounts for 28.3% [1]. Extra-long highway tunnels have a busy traffic flow compared to normal tunnels, and the chances of fire and hazards are greater. In 1999, a fire broke out in a truck loaded with butter and flour in the Mont Blanc tunnel (11.6 km) connecting France and Italy, killing 41 people, destroying 36 cars, and burning for 53 h [2]. In 1999, a fire broke out in the Tauern Tunnel (6.4 km) in Austria due to a series of vehicle rear-end collisions, killing 12 people and injuring 49 others [3]. In 2001, the St. Gotthard Tunnel in Switzerland (16.32 km) was the scene of a fire caused by a collision between two trucks, resulting in 11 deaths [4]. Recent tunnel fires in the country include the Xuefeng Tunnel (7.023 km) fire in 2020 and the Maoliling Tunnel fire (3.59 km) in 2019, with the former causing two deaths and the latter causing five deaths [5]. The extra-long road tunnel itself is a long, narrow, and nearly

enclosed structure [6]. The smoke from the fire is difficult to vent and spreads over a long distance in the tunnel [7]. The smoke contains a large amount of CO and other toxic gases, which can lead to death by poisoning or asphyxiation if large amounts of smoke accumulate in the travel space [8]. Visibility in the tunnel is also reduced by the smoke flow, hindering the evacuation and rescue of personnel. The characteristics of fires in extra-long highway tunnels pose a huge challenge to evacuating people.

Most of the operational ventilation in long-distance road tunnels is mechanical ventilation, which can be divided into longitudinal, semi-transverse, full transverse, and hybrid ventilation [9]. In China, long-distance tunnels mainly use jet fans for longitudinal ventilation, with the direction of airflow in line with the direction of traffic [10]. Some tunnels larger than 10 km are equipped with a number of shafts or inclined shafts to supplement the air volume and discharge the exhaust gases to meet the requirements of long-distance air supply. Typical representatives are Zhongnanshan Tunnel, Baojiashan Tunnel, and Chengkai Tunnel [11]. In case of fire, the smoke is induced by longitudinal ventilation, so that the smoke is discharged from the nearest shaft downstream, which greatly reduces the distance of smoke spread. This type of ventilation is simple in structure, less expensive to operate and maintain, and can effectively utilize the piston wind generated by moving cars. Two types of evacuation modes are used in extra-long road tunnels: horizontal evacuation and vertical evacuation [12]. The horizontal evacuation mode is applicable to most of the mountainous tunnels and some of the cross-harbor tunnels. When a disaster occurs on one side of the tunnel, trapped people and vehicles are evacuated to the other side of the tunnel through the pedestrian cross-passage and vehicle cross-passage in the middle of the tunnel on both sides [13], such as Chengkai Tunnel and Qinling-Tiannanshan Tunnel. The longitudinal evacuation mode is applicable to large shield tunnels, mainly underwater shield tunnels, where trapped people are evacuated to the lower passage of the tunnel through evacuation stairs or slides [14]. Representative tunnels are Shanghai Yangtze River Tunnel and Wuhan Yangtze River Tunnel. In this paper, Chengkai Tunnel is chosen as a study case of tunnel fire evacuation precisely because of its representative ventilation method and evacuation mode. Its section size is a two-lane-sized three-centered circular arch, similar to most mountain tunnels.

The study of the evacuation of tunnel fire personnel is a complex science with a high degree of integration of multiple fields and disciplines, involving numerous uncertainties, and can be divided into four areas according to its research methods: accident investigation and case study analysis, physical experiments, computational model research, and personnel behavior investigation research [15]. With the rapid development of computer technology, scholars have conducted qualitative or quantitative research on personnel evacuation behavior by establishing fire personnel evacuation models [16], partly based on coupled psychological, physiological, and behavioral models of tunnel fire personnel evacuation, and some tunnel fire personnel evacuation movement models based on virtual reality (VR) and augmented reality (AR) coupling have started to be proposed [17]. Such evacuation models can be divided into two categories: hydraulic models for personnel evacuation (continuous medium models) and personnel collision models (discrete medium models) [18], and this type of research has helped scholars to achieve numerous results. Enrico Ronchi et al. [19] compared evacuation models such as Evac, STEPS, and Pathfinder and concluded that the main factors leading to differences in model calculations were the use of unfavorable pre-evacuation times and the exit selection process in low visibility conditions. Caliendo et al. [20] conducted simulations using the STEPS personnel evacuation model associated with a CFD model simulating a fire and found that evacuation time was mainly influenced by walking time and, to a lesser extent, by pre-movement time. The presence of an alarm system reduced the evacuation time for most tunnel users. Seike et al. [21] proposed a one-dimensional evacuation simulation method for quantitative assessment of fire safety in road tunnels, defining various smoke environment levels as a function of longitudinal position and time for different longitudinal gradients, fire intensity, and pre-evacuation times.

The key to determining whether people can be successfully evacuated is the available safe egress time (ASET) and required safe egress time (RSET) [22]. For tunnel fires, the ASET depends on the size of the fire, cross-sectional dimensions, wind speed, and the slope rate of the tunnel; the RSET depends on the layout of the cross passage, the number of people, the speed of movement, and the familiarity with the tunnel. In this paper, a typical extra-long highway tunnel—Chengkai Tunnel—is used as an engineering model, and longitudinal wind speed, the number of personnel, and cross-passage width are selected as variables for the study, and their ASET and RSET are derived by simulating fire scenarios and evacuation scenarios through FDS and Pathfinder software. The innovation of this paper is to propose the concept of safe evacuation reliability, which is used to evaluate the longitudinal wind speed on evacuation impact. The results of this study can be used to develop scientific fire evacuation strategies and can be used as a reference for designers and operators of very long road tunnels with the same ventilation pattern and cross-sectional dimensions.

## 2. Model Establishment and Working Condition Setting

### 2.1. Modeling Parameters

In this paper, Chengkai Tunnel is selected as the engineering background for the study of tunnel fires. Chengkai Tunnel is the longest highway tunnel in Chongqing, with busy traffic flow and a risk of vehicle fires. It is located on the highway from Chengkou to Kaixian and is 11,489 m long in the left lane and 11,456 m long in the right lane, and is ventilated longitudinally by a combination of shafts and jet fans [23]. The shaft divides the tunnel into three sections, each with a length of 3 km to 4 km. The shafts are connected to the tunnel through liaison shafts to provide fresh air and discharge exhaust gases. Figure 1 shows the ventilation diagram of Chengkai Tunnel, and the blue arrows show the direction of wind flow. When a fire occurs in the tunnel, the smoke flow is discharged from the tunnel through the exhaust shaft downstream of the fire to reduce the distance of smoke flow pollution and accelerate the smoke flow discharge. We used Pyrosim fire dynamics software to build a tunnel fire simulation model based on the actual tunnel situation, which is a single-sided tunnel, including the exhaust shaft and the contact shaft. The model was moderately simplified compared to the actual tunnel.

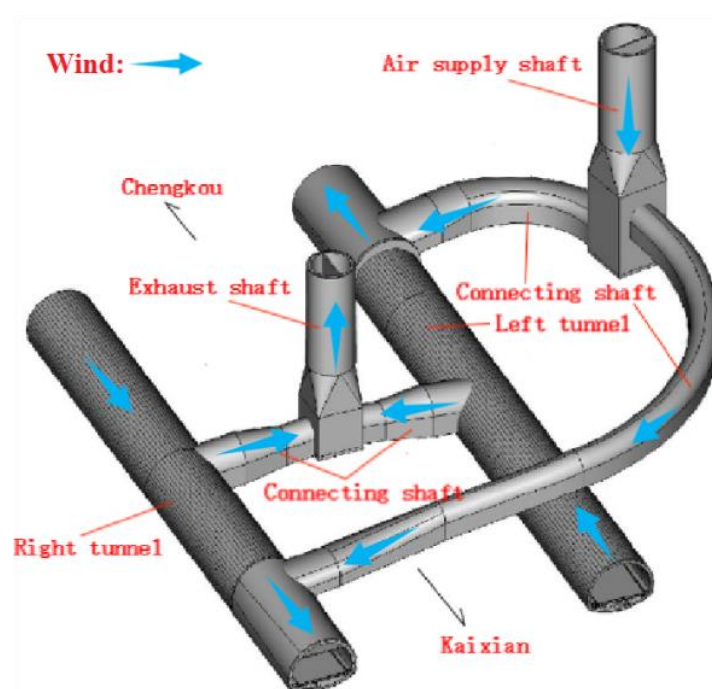


Figure 1. Schematic diagram of wind flow in Chengkai Tunnel.

The length of the tunnel model is 900 m. Due to the limitation of the simulation efficiency of the FDS software, it takes an extremely long time to simulate the complete section of the tunnel model. The fire scenario envisioned in this paper is a vehicle blockage in the tunnel that causes a fire, and the smoke characteristics along the evacuation path of people are mainly analyzed, so a 900 m long tunnel model is sufficient. The overall dimensions of the tunnel model are shown in Figure 2, and the detailed dimensions are shown in Figure 3. The cross-section of the tunnel model is a three-centered arch with a net height of 7.2 m and a net width of 10.75 m. Passages with a width of 1 m and a height of 0.3 m are set on both sides of the tunnel. The exhaust shaft is set at a distance of 850 m from the initial end of the tunnel with a height of 50 m. It is connected to the tunnel through a liaison shaft. The cross-sectional areas of the exhaust shaft and the liaison shaft were 38 m<sup>2</sup> and 34 m<sup>2</sup>, respectively. The surface properties of the model were set to be layered. The inner wall is concrete with a thickness of 0.25 m. The concrete density is set to 2300 kg/m<sup>3</sup>, the thermal conductivity is set to a factor of 1.2 W/(m·K), and the specific volume is set to 1100 J/(kg·K). The rest is the rock layer. The initial end of the tunnel model is set as the air inlet, the end is set as the opening, the top of the exhaust shaft is set as the exhaust port, and the wind flow direction is the blue arrow in Figure 3. The initial temperature inside the model is 20 °C. To analyze the smoke characteristics along the evacuation path of the personnel, temperature, visibility, and CO concentration slices were set up at the height of the personnel (2 m above ground level). Smoke concentration slices were set at the mid-axis of the tunnel and 200 m downstream of the fire source to observe whether the smoke flow reversed back and the distribution of the smoke flow in the cross-section.

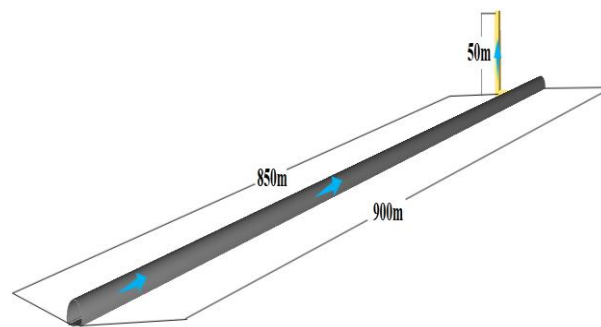


Figure 2. Overall dimensions of the tunnel model.

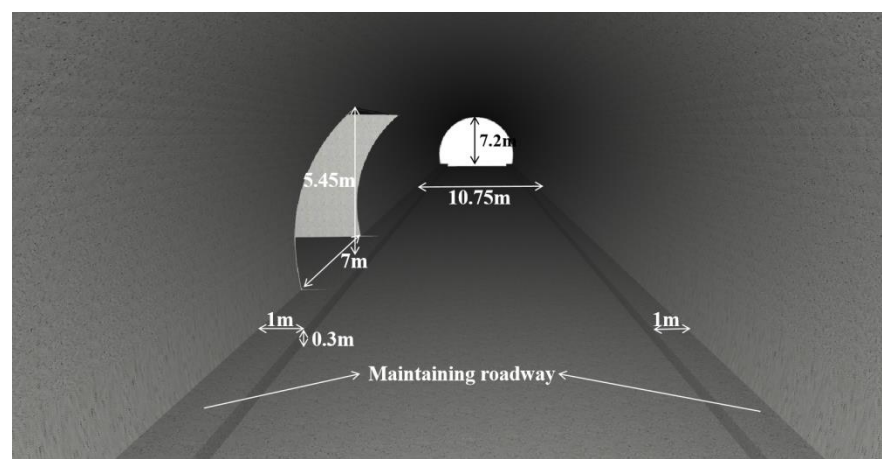


Figure 3. Detailed dimensions of the tunnel model.

## 2.2. Fire Source Setting and Grid Division

According to the Highway Tunnel Ventilation Design Rules (JTG/T D70/2-02-2014), Chengkai Tunnel is a double-hole unidirectional extra-long highway tunnel, and the maximum firepower it can cope with is 30 MW. Additionally, according to the typical vehicle fire

standard of NFPA-502-2020, a 30 MW fire is equivalent to a large truck fire. Therefore, the total fire source size of the tunnel model is set to 10 m × 2.5 m, the fire source growth rate is  $t^2$  ultra-fast fire growth model, and the time to reach the maximum exothermic power is 400 s. The fire source location is 400 m from the initial end of the tunnel, in the middle of the lane, and close to the ground. According to the fire law on fire evacuation time, 6 min is allowed for civil buildings with fire resistance class I and II and 5 min is allowed for public buildings. Considering that the tunnel is a long, narrow, and a nearly closed large space structure, the simulation time of the fire should be greater than the necessary safe egress time of the personnel, and the simulation time of the fire is finally determined to be 600 s.

Grid size selection is critical for fire simulations and has a large impact on the accuracy and time consumption of the simulation. The larger the grid size, the longer the simulation will take, but it will affect the accuracy of the values and the detail of the model. The smaller the grid size, the higher the accuracy of the simulation, but it will consume a lot of time. McGrattan [24] proposed that the ratio of the characteristic diameter of the fire source to the grid diameter  $D^*/\delta x$  represents the precision of the fire source grid. The larger the value, the more accurate. The expression for  $D^*$  is:

$$D^* = \left[ \frac{Q}{\rho_0 C_p T_\infty \sqrt{g}} \right]^{\frac{2}{5}} \quad (1)$$

In the formula,  $D^*$  is fire characteristic diameter, m;  $Q$  is heat release rate, kw;  $\rho_0$  is the ambient air density,  $\text{kg}/\text{m}^3$ ;  $C_p$  is the specific heat of air at constant pressure,  $\text{kJ}/(\text{kg}\cdot\text{K})$ ;  $T_\infty$  is the ambient air density, K; and  $g$  is gravitational acceleration,  $\text{m}/\text{s}^2$ .

According to the FDS guidebook recommendations [25], the simulation results are more accurate when the grid size is  $0.1 D^*$ , so a fire size of 30 MW is brought into the formula calculation, and the resulting grid size is 0.37 m. For best accuracy, the cell dimensions should ideally be close in length in all three directions. Therefore, in order to compare the effects of different grid sizes on simulation accuracy, four cubic grids of 0.25 m, 0.35 m, 0.40 m, and 0.50 m were selected for grid independence tests under a 30 MW fire source to compare their temperature differences. Figure 4 shows the temperature variation at a 2 m height under different grids. In the figure, it can be seen that the temperature at a 2 m height gradually increases with the increase in grid size, but the overall variation is not very different and the temperature variation curve can converge. Considering the accuracy and efficiency of the simulation, the encrypted area is between the fire source location and 200 m downstream and a 0.25 m cubic grid is used, while a 0.5 m cubic grid is used for the other areas. There are 17,788,416 grids in the whole tunnel model.

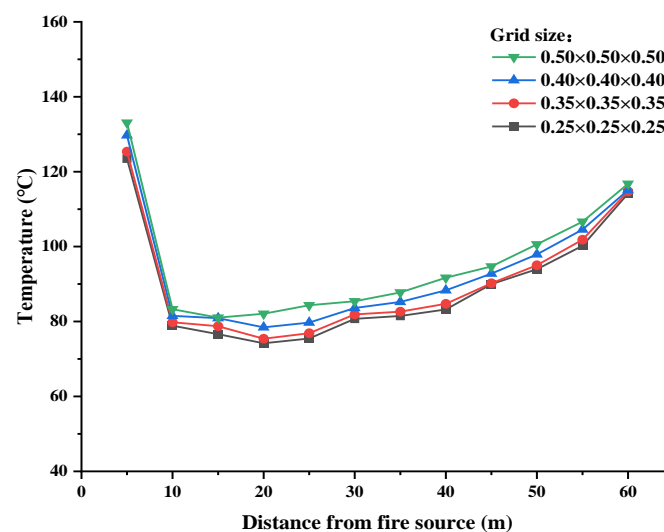


Figure 4. Temperature at a 2 m height for different grid sizes.

### 2.3. Setting of Fire Scenarios

In longitudinally ventilated tunnels, the longitudinal wind velocity has a significant impact on fire smoke dispersion. Longitudinal winds will reduce the temperature of the fire area in the tunnel, but they can also disrupt the uniform distribution of the smoke layer and cause the smoke flow to descend prematurely to personnel height. If the smoke layering structure can be maintained at the beginning of a tunnel fire, so that the toxic and harmful hot smoke is kept in the upper space of the tunnel, favorable conditions can be created for personnel evacuation and escape. This paper focuses on analyzing fire scenarios with different longitudinal wind speeds and exploring the effect of wind speed on personnel evacuation laws. The critical wind speed can prevent the smoke from retreating and ensure the safe evacuation of people in the upper part of the fire and the fire rescue personnel to the fire scene. Wu and Bakar [26] conducted another series of small-scale experiments, taking into account different tunnel cross-sections and using the hydraulic diameter instead of the tunnel height in the equation, with the following equation for the critical wind speed.

$$V_c' = \begin{cases} 0.40, Q' > 0.20 \\ 0.40 \left( \frac{Q'}{0.20} \right)^{\frac{1}{3}}, Q' \leq 0.20 \end{cases} \quad (2)$$

$$Q' = \frac{Q}{\rho_0 c_p T_0 g^{\frac{1}{2}} \bar{H}^{\frac{5}{2}}}, V_c' = \frac{V_c}{\sqrt{g \bar{H}}}$$

where  $V_c'$  is dimensionless ventilation velocity.  $V_c$  is critical wind speed, m/s;  $Q$  is total heat release rate, kW;  $Q'$  is dimensionless heat release rate;  $c_p$  is the thermal capacity of air, kJ/kg K;  $\rho_0$  is ambient density, kg/m<sup>3</sup>;  $T_0$  is the temperature of the wind flow before the tunnel fire, K;  $g$  is the acceleration of gravity, m/s<sup>2</sup>; and  $\bar{H}$  is hydraulic diameter, m.

The hydraulic diameter of Chengkai Tunnel is 8.28 m, the ambient temperature is 20 °C, the power of the fire source is 30 MW, and the critical wind speed is calculated as 3.12 m/s, according to the above formula. In this paper, the longitudinal wind speed range of the tunnel fire scenario is set from 0.0 m/s to 4.0 m/s, and a total of nine wind speeds are selected. The exhaust vent meets the requirement that the wind speed is not greater than 8 m/s combined with the area of the exhaust vent, which is 38 m<sup>2</sup>; so, the vertical shaft exhaust volume is set to 300 m<sup>3</sup>/s. The fire scenarios settings for the tunnel are shown in Table 1.

**Table 1.** Tunnel fire scenarios.

Scenarios	Fire Source Power/MW	Longitudinal Wind Speed / (m/s)	Shaft Exhaust Volume/(m <sup>3</sup> /s)
A1~A9	30	0.0; 0.5; 1.0; 1.5; 2.0; 2.5; 3.0; 3.5; 4.0;	300

### 2.4. Setting of Evacuation Scenarios

In this paper, we assume that a vehicle fire has occurred resulting in a blockage of vehicles downstream of the fire source and trapped persons walk to the crosswalk exit to the other side of the tunnel. The various types of trapped vehicles are replaced by small rooms of different sizes in the lane, where the occupants are drivers and passengers. The vehicle parameters are shown in Table 2. The tunnel personnel evacuation model is shown in Figure 5. The personnel in the vehicle escape through two crosswalks, the distance between the two crossings is 300 m, and the length of the crossings is 50 m. Factors affecting the evacuation speed of personnel in a tunnel fire include personnel density, smoke, environment, lighting, physiological age differences of personnel, obstacles, etc. PIARC recommends that the movement speed of personnel in a tunnel during a fire be taken as 0.5 m/s~1.5 m/s. In this evacuation model, the personnel movement velocity obeys a normal distribution of  $1.25 \pm 3\sigma$  with  $\sigma = 0.1$  m/s [27]. The tunnel personnel

evacuation scenario configuration is shown in Table 3. The evacuation scenarios with a different number of people were simulated by adjusting the full load rate of vehicles, as in scenarios R1~R3. The widths of pedestrian crossings were set from 2 m to 4 m to study the effects of different widths of crosswalks on evacuation efficiency, as in scenarios R3~R7.

**Table 2.** Vehicle parameters.

Vehicle Type	Large Bus	Medium Bus	Minibus	Large Truck	Medium Truck	Minivan
Distribution ratio/%	1.6	6.3	76.2	1.6	4.8	9.5
Vehicle length/m	11.5	7.1	5	14	9	5.5
Vehicle width/m	2.5	2.2	1.8	2.8	2.5	2.2
Vehicle spacing/m	2.0	1.5	1.5	2.0	1.5	1.5
Full load capacity	55	20	5	2	2	2
Trapped quantity	1	4	48	1	3	6

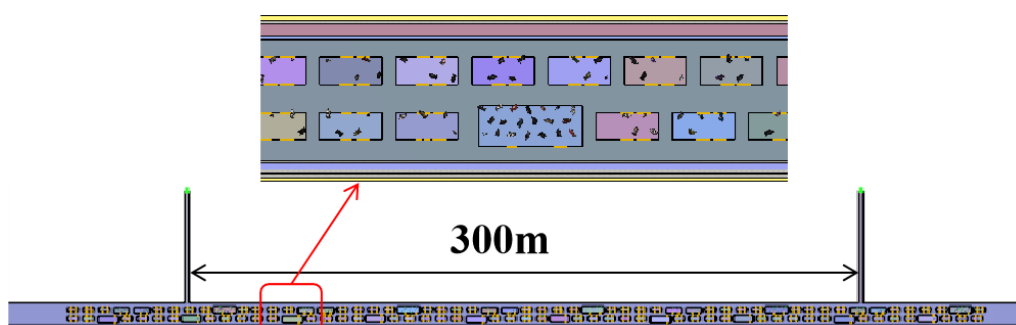


**Figure 5.** Tunnel evacuation model.

**Table 3.** Evacuation scenarios of tunnel personnel.

Scenarios	Full Load Rate/%	Number of Evacuees/Person	Width of Cross Passage/m
R1	50%	191	2.0
R2	75%	312	2.0
R3	100%	395	2.0
R4	100%	395	2.5
R5	100%	395	3.0
R6	100%	395	3.5
R7	100%	395	4.0

### 3. Analysis of Simulation Results

#### 3.1. Analysis of the ASET

The ASET is the maximum evacuation time allowed when a fire has progressed to the point where it poses a danger to people. High temperatures, toxic gases, and low visibility due to smoke are the main factors affecting the evacuation of personnel. Therefore, ambient temperature, CO concentration, and visibility are selected as criteria for judging the safe evacuation of personnel at personnel height (2 m above ground level). Research shows that when the human body is directly exposed to an ambient temperature of 60 °C, there is strong discomfort within a few minutes, so 60 °C is selected as the safety boundary condition of the temperature [28]. When CO concentration reaches 2000 PPM (0.2%), the human body will experience headaches, vomiting, and blurred vision within 20 min, which can be fatal within 1 h; so, 0.2% CO concentration is selected as the safety boundary condition [29]. The Australian guide for fire engineers gives a minimum visibility table applicable to both small and large spaces. Road tunnels are narrow and large spaces, so the

safety boundary condition for visibility is 10 m [30]. The safety boundary conditions for the evacuation of people in a tunnel fire are shown in Table 4. When the temperature, CO concentration, and visibility of an area in the tunnel reach the safety boundary condition first, the time until the fire occurs is the ASET.

**Table 4.** Safety boundary conditions for personnel evacuation.

Environmental Temperature	Visibility	CO Concentration
$\leq 60$ °C	$\geq 10$ m	$\leq 0.2\%$

In this paper, fire scenario A1 with no longitudinal wind speed is used as an example to analyze the cloud plots of CO concentration, temperature, and visibility at personnel height, as shown in Figure 6, to derive the ASET for this scenario.

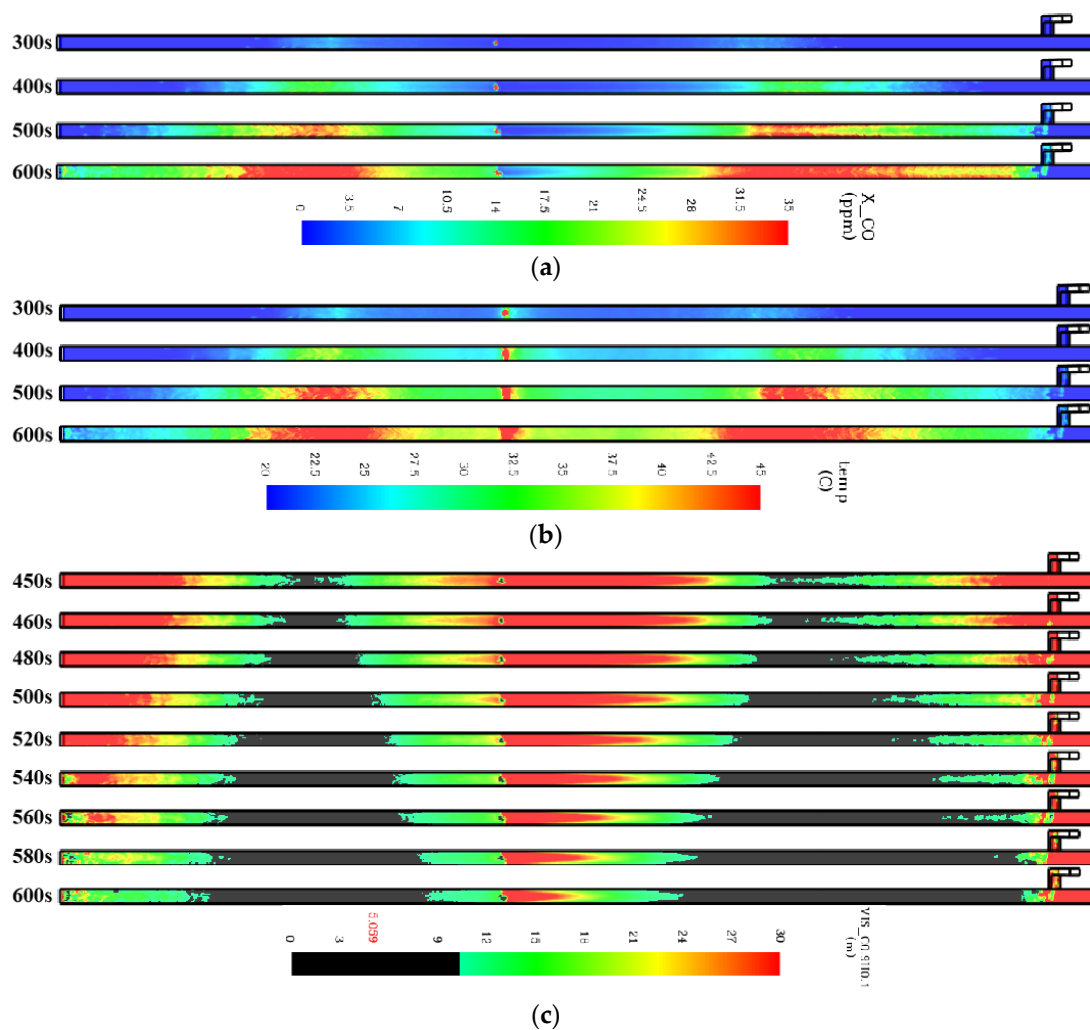


**Figure 6.** Change in smoke characteristics in scenario A1. (a) CO concentration; (b) temperature; (c) visibility.

In Figure 6a,b, it can be seen that there is no significant change in CO concentration and temperature at the characteristic height of personnel in the tunnel before 300 s. The maximum CO concentration and maximum temperature within the 600 s moment are 35 PPM and 45 °C, respectively, which are within the safety boundary conditions. The high-temperature area and high-CO concentration area (red part in the figure) are distributed in 101 m~200 m upstream of the fire source and 181 m~309 m downstream of the fire source. Although the distribution area is large, it does not pose a threat to the evacuation

of personnel. Therefore, in the A1 scenario, temperature and CO concentration are not the main factors affecting the available safe evacuation time.

The black part in Figure 6c is the “area” where the visibility is lower than the safety boundary condition, which is called the hazardous area in this paper. At 450 s, the hazardous area starts to form gradually upstream and downstream of the fire source. At 460 s, a hazardous area of 41 m is formed upstream of the fire source, and a hazardous area of 42 m is formed downstream of the fire source. From 460 s to 600 s, the danger zone gradually expands, and 600 s, 187 m, and 285 m danger zones are formed upstream and downstream of the fire source, respectively. The downstream hazard area was distributed between 154 m and 439 m from the fire source, and the upstream hazard area was distributed between 64 m and 251 m from the fire source. Due to the installation of exhaust shafts downstream of the fire source, the smoke sinking phenomenon is more serious than upstream, but the visibility downstream of the smoke exhaust is good. Most of the smoke flow can be discharged through the shaft, and the smoke can be well-isolated in the fire zone. Therefore, in the A1 scenario, the factor affecting the ASET is visibility, and the ASET is 450 s for both upstream and downstream of the fire source. It is worth noting that the first hazardous zone is not the closest place to the fire, but a certain distance away from the fire. The reason for this phenomenon is that the smoke temperature near the fire source is higher. Under the action of buoyancy, the smoke mostly moves in the tunnel vault. After a distance of the spread, the smoke and the tunnel wall heat exchange and cold air mix, resulting in a reduced temperature, and the height of the smoke layer drops to the height of the human eye characteristics, resulting in reduced visibility.

Following the analysis method of scenario A1, the ASET and the influencing factors of the upstream and downstream of the fire source under different wind speeds were counted separately, as shown in Table 5. In the table, it can be seen that visibility is the main factor affecting the ASET upstream of the fire source, and the ASET increases gradually with the increase in wind speed. When the wind speed increases to 2 m/s, the ASET is  $\geq 600$  s and remains constant. For the downstream of the fire source, as the longitudinal wind speed increases, the factor affecting the ASET changes from visibility to temperature, and the ASET first increases and then decreases. When the wind speed is 2.5 m/s, the ASET is the largest, 590 s.

**Table 5.** ASET statistics at different wind velocities.

Longitudinal Wind Velocity/(m/s)	Upstream of the Fire		Downstream of the Fire Source	
	Influence Factor	ASET/s	Influence Factor	ASET/s
0.0	VIS	450	VIS	450
0.5	VIS	460	VIS	475
1.0	VIS	530	VIS	550
1.5	VIS	540	VIS	560
2.0	/	/	VIS	580
2.5	/	/	VIS	590
3.0	/	/	TEMP	520
3.5	/	/	TEMP	490
4.0	/	/	TEMP	480

When the wind speed reaches 2 m/s, there is no hazardous area upstream of the fire source compared to when the wind speed reaches the critical wind speed. Figure 7 shows the side view of the tunnel smoke concentration at different wind speeds. As can be seen in the figure, when the wind speed is 2 m/s, the smoke layer remains at a certain height and does not drop to the height of the personnel, although the smoke flow upstream of the fire source reverses a distance of 150 m. Visibility is always above the safety threshold. With the increase in wind speed, the distance of smoke reverse retreat gradually decreases. At the same time, the increase in longitudinal wind speed leads to faster smoke flow movement

and smoke flow overflowing out of the exhaust shaft. When the wind speed is greater than or equal to 2 m/s, the flue gas will overflow the shaft.

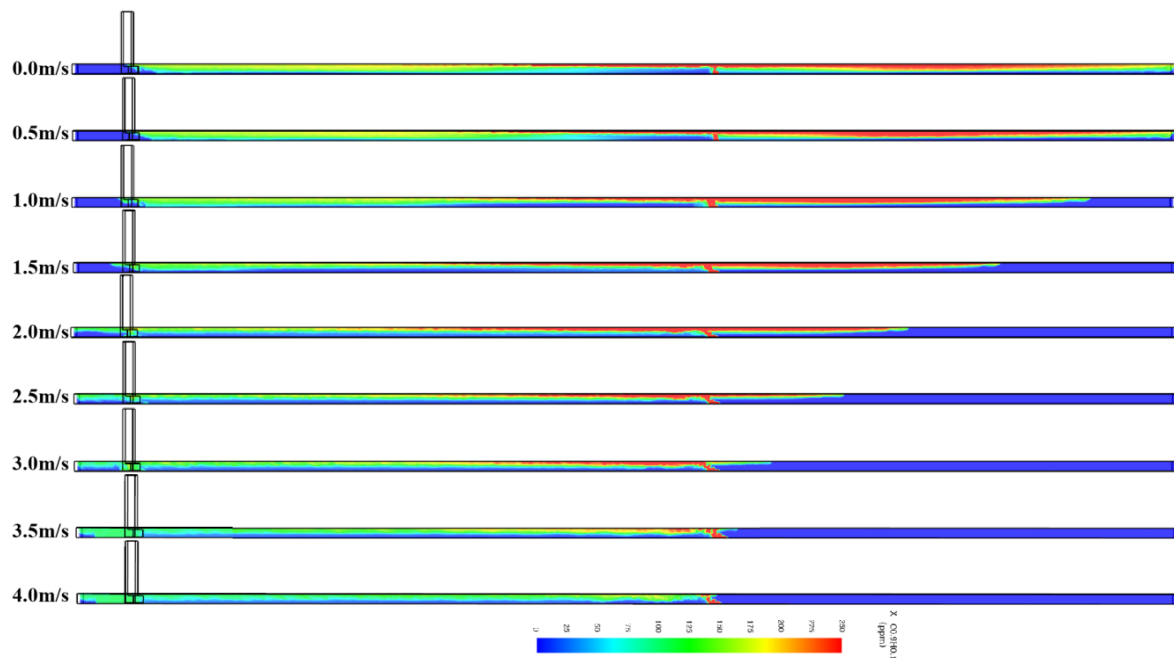


**Figure 7.** Side view of tunnel smoke concentration at 600 s.

The stability of the fire smoke flow as a buoyancy-driven stratified flow is controlled by two main factors. One is that because the temperature is higher than the ambient air temperature, the smoke flow is subject to its own thermal buoyancy, which tends to maintain this stratified structure. The second is the presence of longitudinal winds in the tunnel, which shear with the flue gas layer at the horizontal interface. This mixed shear effect tends to destabilize the flue gas layer and destroy this layered structure [31]. The destructive effect of longitudinal wind speed on the smoke-layered structure downstream from the fire source can be seen in Figure 8.

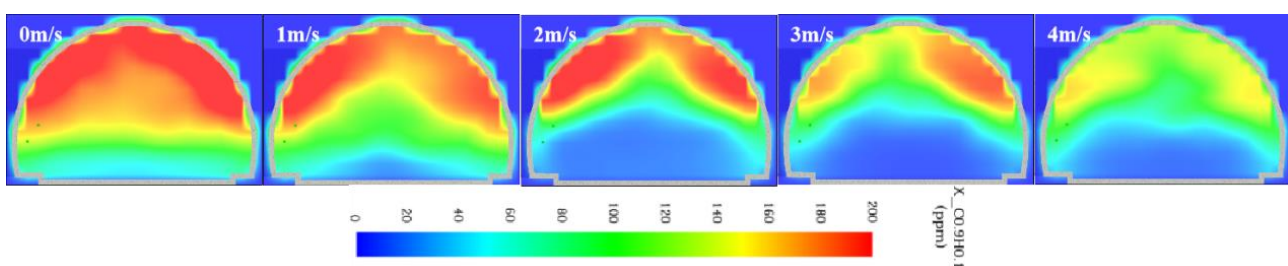


**Figure 8.** Smoke concentration clouds in the cross-section downstream from the fire source.

As shown in Figure 8, the height distribution of the smoke layer under no longitudinal wind speed is uniform, the smoke concentration dividing line is approximately parallel to the horizontal direction, and the smoke almost fills the whole section. With the increase in longitudinal wind speed, the height of the smoke layer is low on both sides and high in the middle, and the smoke concentration dividing line is irregularly curved. At the same time, the smoke concentration in the tunnel cross-section decreases. Therefore, when the wind speed is small, the smoke concentration at the height of the personnel downstream of the fire source is higher and the ASET is affected by visibility. As the wind speed increases, the height of the smoke layer rises to the personnel height and visibility is no longer a factor affecting the ASET. The increase in wind speed leads to the increase in flame angle and the enhancement of thermal radiation at human height, which makes the downstream

temperature of the fire source rise and exceed the safety critical value. Temperature becomes a factor affecting the ASET at high wind speeds.

### 3.2. Analysis of the RSET

The RSET is the minimum time for all personnel to evacuate to the safe area. As shown in Figure 9, it consists of three parts: personnel perception time ( $t_{per}$ ), personnel response time ( $t_{rsep}$ ), and personnel evacuation movement time ( $t_{move}$ ). The difference value of the ASET and RSET is the safety margin, and the larger the safety margin, the more reliable the reaction system is.

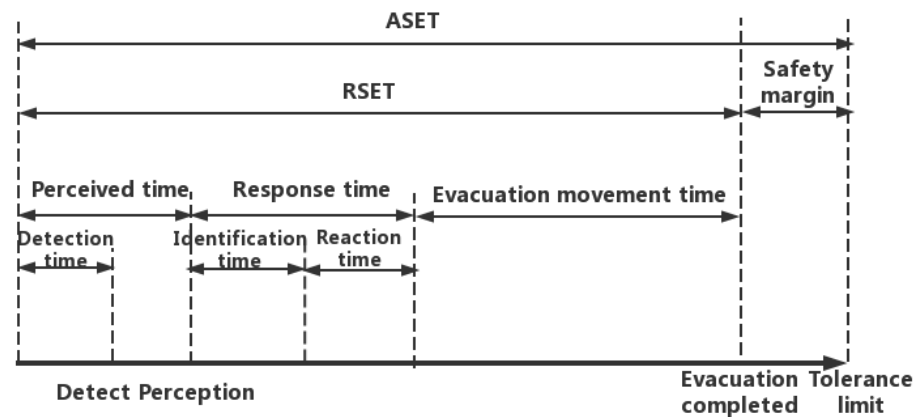


Figure 9. Composition of the RSET.

The fire in the tunnel is mainly a vehicle fire because the fire source growth curve is a  $t^2$  curve. The power of the fire source is small in the early stage, which is not easy to cause people to notice, and the personnel perception time is uniformly set to 60 s. When the trapped people hear the tunnel alarm sound, there will be a pre-action time. During this time people will carry their belongings, observe the surrounding environment, notify their entourage, etc., and then go to the escape route with the flow of people. The response time for different people and different  $t_{rsep}$  is set to 30 s. People's evacuation movement time,  $t_{move}$ , is calculated through Pathfinder software.

Figure 10 shows the change in the number of people in the tunnel with time for different evacuation numbers.  $t_{move}$  is 380 s, 510 s, and 650 s for scenarios R1, R2, and R3, respectively. A hundred seconds after the fire broke out, the crowd began to leave the tunnel. The change curves of the number of people in the three evacuation scenarios are basically parallel, which indicates that the average evacuation speed of the crowd is basically the same, and the total evacuation time is positively correlated with the number of people.

During the evacuation process, bottleneck effects occur at key areas, such as stairway entrances and access exits. As shown in Figure 11, a group of people crowded at a bottleneck will accumulate and stay at the "bottleneck" for a long time, which will lead to a serious decrease in evacuation efficiency and increase the evacuation movement time of people. To study the effect of pedestrian crossing width on evacuation efficiency, a scatter plot for each person is plotted with evacuation movement time as the horizontal coordinate and blockage time as the vertical coordinate. The expression of blockage time was fitted according to the scatter plot, and the results are shown in Figure 12.

In Figure 12, it can be seen that there is a power function relationship between blockage time and evacuation movement time, and the blockage time increases longer with the increase in evacuation movement time. When the evacuation movement time is 650 s, the blockage time is more than 160 s, accounting for 24.6% of the evacuation time. We use the exponent of the power function relationship as the "blockage index" to measure the severity of the blockage. The larger the blockage index is, the more serious the blockage is and the lower the evacuation efficiency is, and vice versa. As the width of the evacuation

channel increases, the blockage index gradually decreases. The relationship shows that the blockage index decreases from 2.26 to 2.10 when the width of the pedestrian crossing increases from 2.0 to 4.0 m. This indicates that increasing the width of the tunnel crossing will reduce the blockage during evacuation and improve the efficiency of evacuation. This also provides a solution for tunnel designers to improve the safety of the tunnel.

According to the composition of the RSET, the RSET of scenarios R1, R2, and R3 are 460 s, 630 s, and 760 s, respectively. The safety margins can be obtained by the difference between the RSET and ASET, which was mentioned at the beginning of Section 3.2, and the value of the ASET was obtained in Table 5. Taking the longitudinal wind speed of 1.5 m/s as an example, the safety margin of scenario R1 is 100 s, while the safety margins of scenarios R2 and R3 are  $-70$  s and  $-200$  s. As the number of evacuees increases, the safety margin decreases by a negative number, indicating that it is not possible to evacuate all the individuals safely at this time. However, considering the inconsistent RSET of numerous individuals, the RSET reflects the longest evacuation time in the group, which is not a good representation of the time for most people to complete the evacuation. Therefore, the concept of safety margin is not applicable in the evacuation of tunnel personnel, and the safe evacuation reliability is a better indication of the relationship between the ASET and RSET.

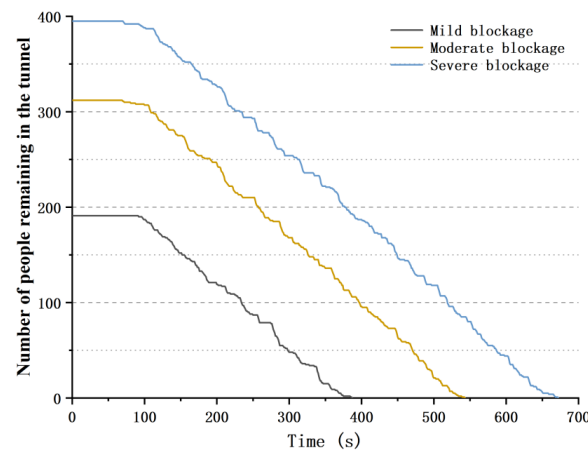


Figure 10. Changes in the number of people remaining in the tunnel.

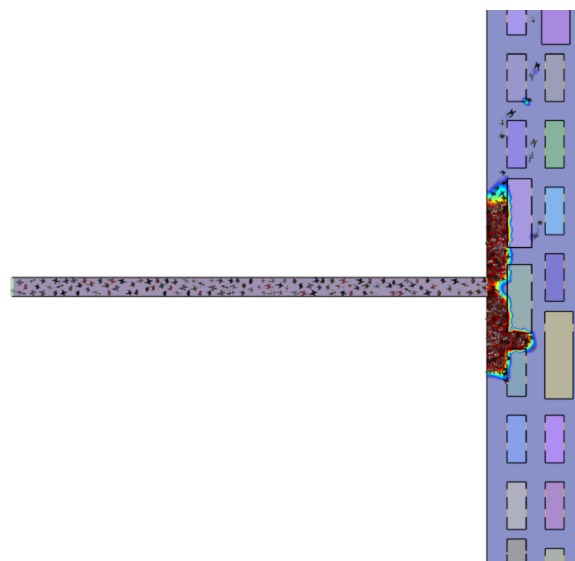


Figure 11. Bottleneck effect in the evacuation process.

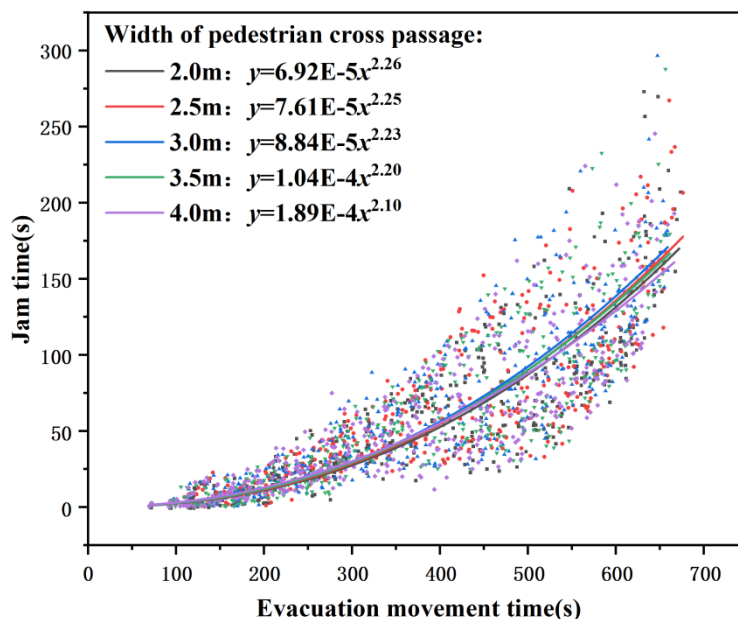


Figure 12. Jam time distribution.

### 3.3. Analysis of Safety Evacuation Reliability

In systems engineering, reliability is the probability that a product or system will perform its intended function at a specified time and under specified conditions [32]. In personnel evacuation studies, the reliability of safe evacuation of personnel refers to the probability that all personnel can be safely evacuated in a fire environment. When the RSET ( $t_R$ ) of personnel is less than the ASET ( $t_A$ ), it can be considered that all personnel can be evacuated safely. The reliability of the safe evacuation of personnel  $R$  can be expressed as:

$$R = P(t_R < t_A) \tag{3}$$

where  $P$  is the probability. The  $t_A$  under different fire scenarios can be obtained in Table 5.  $t_R$  is affected by random factors such as escape distance, building facilities, and personnel response time, and is a random variable which belongs to the probability distribution curve. Set  $f(t_R)$  as the probability density function of  $t_R$ , as shown in Figure 13. The probability that  $t_R$  is less than  $t_A$  is  $R$ .

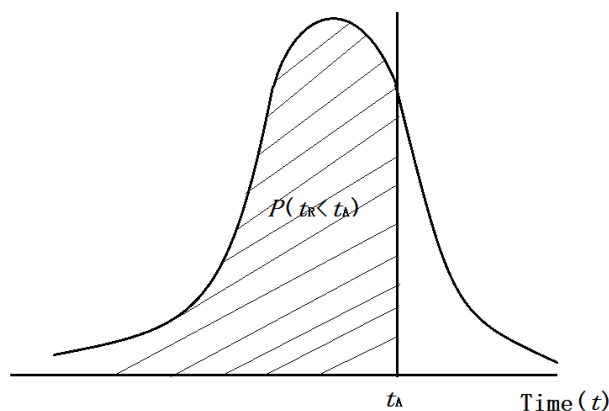


Figure 13. Reliability of personnel evacuation.

We tested the ASET of individuals in scenarios R1, R2, and R3 for normal distribution. To improve the accuracy of the test sample, two simulations of these three scenarios were conducted to obtain 382, 624, and 790 individual evacuation time data, respectively, and then the results of these data were sampled and analyzed. The data were arranged in order

of size, and then the K-S test was performed by SPSS software to test whether the RSET of the personnel conformed to a normal distribution curve. To ensure high confidence in the conclusions obtained, the sample content of the K-S test should be at least 100 [33]. Therefore, the evacuation times for scenarios R1, R2 and R3 were averaged into 128, 156 and 158 groups, and a random sample of data from each group was selected to form the test. The results of the test are shown in Table 6.

**Table 6.** K-S test results of personnel evacuation time.

Evacuation Scenarios	Sample Size	Normal Distribution Parameter Mean Value	Normal Distribution Parameter Standard Deviation	Inspection Statistics	Progressive Significance (Bilateral)
R1	128	333.67	93.26	0.546	0.672
R2	156	414.06	120.89	0.498	0.796
R3	158	479.43	154.27	0.559	0.664

According to Table 6, the asymptotic significance of the three evacuation scenarios are all significantly greater than 0.05, indicating that all accept the null hypothesis; that is,  $t_R$  obeys a normal distribution, denoted as  $t_R \sim N(\mu, \sigma^2)$ .  $\mu$  is the average evacuation time of personnel.  $\sigma$  is the standard deviation, indicating the dispersion degree of the average evacuation time of personnel. The  $t_R$  probability density function  $f(t_R)$  can be expressed as:

$$f(t_R) = \frac{1}{\sqrt{2\pi}} \sigma e^{-\frac{1}{2} \left( \frac{t-\mu}{\sigma} \right)^2} \quad (0 < t < \infty, 0 < \mu < \infty, 0 < \sigma < \infty) \quad (4)$$

Defined by the normal distribution function, the safety evacuation reliability  $R$  can be expressed as:

$$R = P(t_{\text{alarm}} + t_{\text{resp}} < t_R < t_A) = P\left(\frac{90 - \mu}{\sigma} < \frac{t_R - \mu}{\sigma} < \frac{t_A - \mu}{\sigma}\right) \quad (5)$$

Figure 14 shows the calculation results of safety evacuation reliability under different longitudinal wind speeds. It can be seen in the figure that the safety evacuation reliability of the R1 scenario is significantly higher than that of the other two scenarios due to the small number of evacuees. The safety evacuation reliability upstream of the fire source increases with the increase in the longitudinal wind speed, and the reliability of scenarios R2 and R3 increases significantly. When the wind speed reaches 2 m/s, the safety evacuation reliability remains unchanged, the safety evacuation reliability of R1 is close to 1, and the R2 and R3 scenarios are 0.93 and 0.82. The safety evacuation reliability downstream of the fire source first increases and then decreases with the increase in wind speed. When the longitudinal wind speed is 2.5 m/s, the safety evacuation reliability reaches the highest, and the safety evacuation reliability of the three evacuation scenarios are 0.99, 0.92, and 0.79, respectively. When the longitudinal wind speed increases to 4 m/s, the safety evacuation reliability downstream decreases to 0.94, 0.70, and 0.54, respectively. Whether upstream or downstream of the fire source, the increase in evacuation numbers will reduce the reliability of a safe evacuation. A longitudinal wind speed of 2.5 m/s is the most favorable for personnel evacuation. Excessive longitudinal wind speed reduces the safety evacuation reliability downstream of the fire source, especially when there are many evacuees; the evacuation reliability is only 0.5.

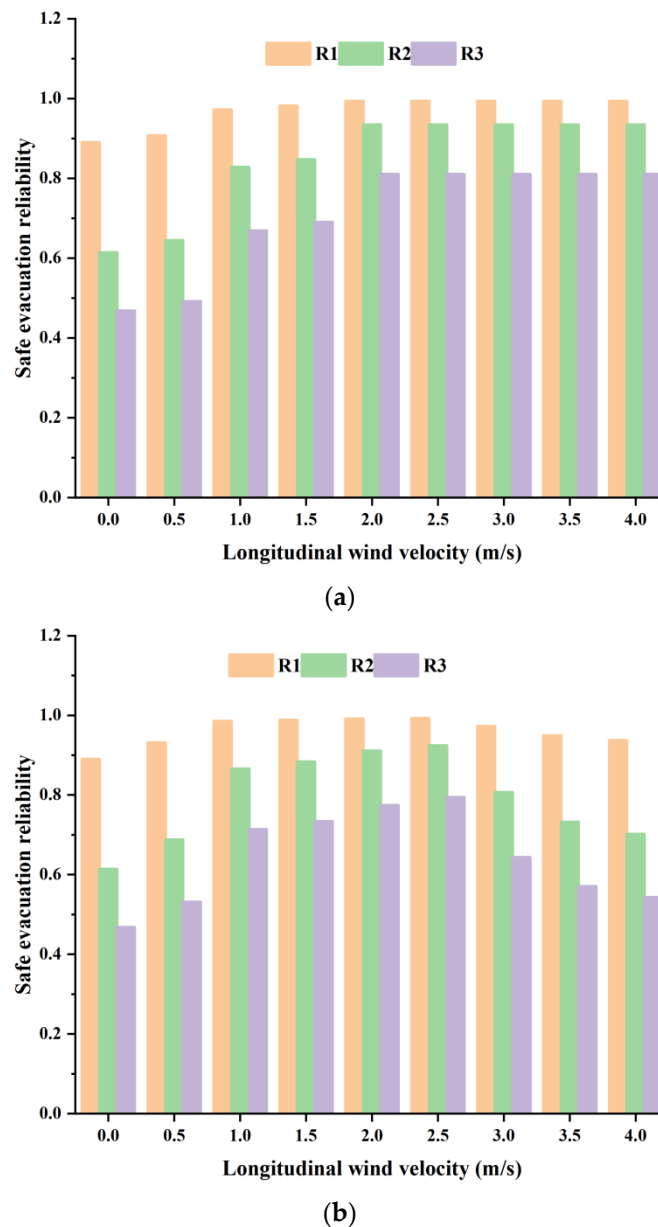


**Figure 14.** Reliability of safe evacuation under different longitudinal wind speeds. (a) Upstream of the fire source. (b) Downstream of the fire source.

#### 4. Conclusions

1. After a fire occurs in an extra-long highway tunnel, the ASET upstream of the fire source is affected by the visibility and increases with the increase in the longitudinal wind speed. When the wind speed increases to 2 m/s, the ASET reaches the maximum and remains unchanged. The ASET downstream of the fire source is affected by visibility when the wind speed is small and affected by temperature when the wind speed is large, and it first increases and then decreases with the increase in wind speed. When the wind speed is 2.5 m/s, the ASET reaches the maximum, which is 590 s. Excessive longitudinal wind speed will make smoke overflow the fire source section.
2. The average evacuation speed of different evacuees is basically the same, and the evacuation movement time is in direct proportion to the number of evacuees. The bottleneck effect is an important reason for the long evacuation time. Increasing the width of the evacuation channel can reduce the time of personnel blockage. The relationship between the blocking time and the evacuation time is a power

function, and its exponent decreases with the increase in the width of the cross passage. Increasing the width of the cross-passage can improve the efficiency of evacuating people, especially when the number of evacuees is high. Therefore, the tunnel designer should design a reasonable cross-passage width according to the traffic flow of the tunnel to improve the evacuation efficiency of the tunnel.

3. Safety evacuation reliability can be a good description of the relationship between the ASET and RSET. The increase in the number of evacuees decreases the reliability of safe evacuation. Combined with the fire scenario in this paper, a longitudinal wind speed of 2.5 m/s is the most favorable for the evacuation of people in Chengkai Tunnel, with a safety evacuation reliability of 0.79, 0.92, and 0.99 for scenarios R1, R2, and R3, respectively. As the wind speed increases, the safety evacuation reliability upstream of the fire source approaches 1. While the safety evacuation reliability downstream of the fire source decreases, the smoke will overflow the exhaust shaft. Therefore, the tunnel operator should maintain a reasonable longitudinal wind speed at the beginning of the fire to provide conditions for evacuation and escape.

**Author Contributions:** Conceptualization, K.W. and J.H.; methodology, K.W.; software, K.W.; validation, K.W., J.H. and R.C.; formal analysis, K.W.; investigation, J.H.; resources, K.W.; data curation, J.H.; writing—original draft preparation, J.H.; writing—review and editing, J.H.; visualization, J.H.; supervision, J.W.; project administration, K.W.; funding acquisition, K.W. All authors have read and agreed to the published version of the manuscript.

**Funding:** This research received funding from the National Natural Science Foundation of China, grant number 52074278 and National Key Research and Development Projects, grant number 2022YFC3004800.

**Institutional Review Board Statement:** Not applicable.

**Informed Consent Statement:** Not applicable.

**Data Availability Statement:** Not applicable.

**Conflicts of Interest:** The authors declare no conflict of interest.

## References

1. Transport, M.O. 2020 Statistical Bulletin on the Development of the Transportation Industry. *Transp. Account.* **2021**, *3*, 92–96.
2. Duffé, P.; Marec, M. Task Force for Technical Investigation of the 24 March 1999 Fire in the Mont Blanc Vehicular Tunnel. Minister of the Interior, Ministry of Equipment, Transportation and Housing, France. 30 June 1999.
3. Leitner, A. The fire catastrophe in the Tauern Tunnel: Experience and conclusions for the Austrian guidelines. *Tunn. Undergr. Sp. Tech.* **2001**, *16*, 217–223. [[CrossRef](#)]
4. Carvel, R.; Marlair, G. A History of Fire Incidents in Tunnels. 2005. Available online: <http://worldcat.org/isbn/0727731688> (accessed on 10 May 2022).
5. Liu, J.; Yang, G.; Wang, W.; Zhou, H.; Hu, X.; Ma, Q. Based on ISM-NK Tunnel Fire Multi-Factor Coupling Evolution Game Research. *Sustainability* **2022**, *14*, 7034. [[CrossRef](#)]
6. Hu, X. Numerical study of the effects of ventilation velocity on peak heat release rate and the confinement velocity in large tunnel fires. *Saf. Sci.* **2021**, *142*, 105359. [[CrossRef](#)]
7. Yao, Y.; Wang, R.; Xia, Z.; Ren, F.; Zhao, J.; Zhu, H.; Cheng, X. Numerical study of the characteristics of smoke spread in tunnel fires during construction and method for improvement of smoke control. *Case Stud. Therm. Eng.* **2022**, *34*, 102043. [[CrossRef](#)]
8. Zhang, J.; Zhou, X.; Xu, Q.; Yang, L. The inclination effect on CO generation and smoke movement in an inclined tunnel fire. *Tunn. Undergr. Space Technol.* **2012**, *29*, 78–84. [[CrossRef](#)]
9. Cong, H.; Bi, M.; Bi, Y.; Li, Y.; Jiang, H.; Gao, W. Experimental studies on the smoke extraction performance by different types of ventilation shafts in extra-long road tunnel fires. *Tunn. Undergr. Space Technol.* **2021**, *115*, 104029. [[CrossRef](#)]
10. Chen, J.; Long, Z.; Wang, L.; Xu, B.; Bai, Q.; Zhang, Y.; Liu, C.; Zhong, M. Fire evacuation strategy analysis in long metro tunnels. *Saf. Sci.* **2022**, *147*, 105603. [[CrossRef](#)]
11. Caroly, S.; Kouabenan, D.R.; Gandit, M. Analysis of danger management by highway users confronted with a tunnel fire. *Saf. Sci.* **2013**, *60*, 35–46. [[CrossRef](#)]
12. Khattri, S.K.; Log, T.; Kraaijeveld, A. Tunnel Fire Dynamics as a Function of Longitudinal Ventilation Air Oxygen Content. *Sustainability* **2019**, *11*, 203. [[CrossRef](#)]
13. Dong, S.; Wang, K.; Jia, C. A Study on the Influence of Rail Top Smoke Exhaust and Tunnel Smoke Exhaust on Subway Fire Smoke Control. *Sustainability* **2022**, *14*, 4049. [[CrossRef](#)]

14. Koch, N.; Niewiadomski, A.P.; Wrona, P. Influence of Light Wavelengths on Visibility in Smoke during a Tunnel Fire. *Sustainability* **2021**, *13*, 11599. [[CrossRef](#)]
15. Zhai, L.; Nong, Z.; He, G.; Xie, B.; Xu, Z.; Zhao, J. Experimental Investigation on the Discharge of Pollutants from Tunnel Fires. *Sustainability* **2020**, *12*, 1817. [[CrossRef](#)]
16. Ronchi, E.; Colonna, P.; Berloco, N. Reviewing Italian Fire Safety Codes for the analysis of road tunnel evacuations: Advantages and limitations of using evacuation models. *Saf. Sci.* **2013**, *52*, 28–36. [[CrossRef](#)]
17. Ronchi, E.; Kinateder, M.; Müller, M.; Jost, M.; Nehfischer, M.; Pauli, P.; Mühlberger, A. Evacuation travel paths in virtual reality experiments for tunnel safety analysis. *Fire Saf. J.* **2015**, *71*, 257–267. [[CrossRef](#)]
18. Gao, R.; Li, A.; Lei, W.; Zhao, Y.; Zhang, Y.; Deng, B. Study of a proposed tunnel evacuation passageway formed by opposite-double air curtain ventilation. *Saf. Sci.* **2012**, *50*, 1549–1557. [[CrossRef](#)]
19. Ronchi, E. Testing the predictive capabilities of evacuation models for tunnel fire safety analysis. *Saf. Sci.* **2013**, *59*, 141–153. [[CrossRef](#)]
20. Caliendo, C.; Ciambelli, P.; Guglielmo, M.L.D.; Meo, M.G.; Russo, P. Simulation of People Evacuation in the Event of a Road Tunnel Fire. *Procedia Soc. Behav. Sci.* **2012**, *53*, 178–188. [[CrossRef](#)]
21. Seike, M.; Kawabata, N.; Hasegawa, M. Quantitative assessment method for road tunnel fire safety: Development of an evacuation simulation method using CFD-derived smoke behavior. *Saf. Sci.* **2017**, *94*, 116–127. [[CrossRef](#)]
22. Schröder, B.; Arnold, L.; Seyfried, A. A map representation of the ASET-RSET concept. *Fire Saf. J.* **2020**, *115*, 103154. [[CrossRef](#)]
23. Storm, A.; Celander, E. Field evacuation experiment in a long inclined tunnel. *Fire Saf. J.* **2022**, *132*, 103640. [[CrossRef](#)]
24. McGrattan, K.; Forney, G. *Fire Dynamics Simulator (Version 6) User's Guide*; Nist Special Publication: Gaithersburg, MD, USA, 2018.
25. Hurley, M.J.; Gottuk, D.T.; Hall, J.R., Jr.; Harada, K.; Kuligowski, E.D.; Puchovsky, M.; Torero, J.L.; Watts, J.M., Jr.; Wieczorek, C.J. *SFPE Handbook of Fire Protection Engineering*; Springer: New York, NY, USA, 2015.
26. Wu, Y.; Bakar, M.Z.A. Control of smoke flow in tunnel fires using longitudinal ventilation systems—A study of the critical velocity. *Fire Saf. J.* **2000**, *35*, 363–390. [[CrossRef](#)]
27. Seike, M.; Lu, Y.; Kawabata, N.; Hasegawa, M. Emergency evacuation speed distributions in smoke-filled tunnels. *Tunn. Undergr. Space Technol.* **2021**, *112*, 103934. [[CrossRef](#)]
28. Ingason, H.; Li, Y.Z.; Lönnemark, A. *Tunnel Fire Dynamics*; Springer: New York, NY, USA, 2014.
29. Zhang, Y.; Li, W.; Rui, Y.; Wang, S.; Zhu, H.; Yan, Z. A modified cellular automaton model of pedestrian evacuation in a tunnel fire. *Tunn. Undergr. Space Technol.* **2022**, *130*, 104673. [[CrossRef](#)]
30. Wang, K.; Cai, W.; Zhang, Y.; Hao, H.; Wang, Z. Numerical simulation of fire smoke control methods in subway stations and collaborative control system for emergency rescue. *Process Saf. Environ.* **2021**, *147*, 146–161. [[CrossRef](#)]
31. Tang, F.; Zhu, Y.; Chen, L. Experimental study on the effect of lateral concentrated smoke extraction on smoke stratification in the longitudinal ventilated tunnel. *Fire Mater.* **2020**, *44*, 1004–1012. [[CrossRef](#)]
32. Ronchi, E.; Nilsson, D.; Modig, H.; Walter, A.L. Variable Message Signs for road tunnel emergency evacuations. *Appl. Ergon.* **2016**, *52*, 253–264. [[CrossRef](#)] [[PubMed](#)]
33. Yan, G.; Wang, M.; Yan, T.; Qin, P. Evacuation speed of human beings in road tunnels at different altitudes. *Tunn. Undergr. Space Technol.* **2022**, *128*, 104651. [[CrossRef](#)]

**Disclaimer/Publisher's Note:** The statements, opinions and data contained in all publications are solely those of the individual author(s) and contributor(s) and not of MDPI and/or the editor(s). MDPI and/or the editor(s) disclaim responsibility for any injury to people or property resulting from any ideas, methods, instructions or products referred to in the content.